ORGANIC THIN FILMS FOR PHOTONICS APPLICATIONS

SEPTEMBER 11–14, 1995
PORTLAND, OREGON

1995 TECHNICAL DIGEST SERIES
VOLUME 21

19960325 108

ORGANIC THIN FILMS FOR PHOTONICS APPLICATIONS
POSTDEADLINE PAPERS

POSTER SESSION, Sept. 11, 1995
Lloyd Center Ballroom - 3:45pm - 5:15pm

PD1   Organic thin films on the 30-kJ OMEGA glass
            laser system, Ansgar W. Schmid, Terrance J.
            Kessler, Kenneth Marshall, Joseph Armstrong,
            Univ. of Rochester, USA ....

PD2   Suppression of multi-photon fluorescence in
            hyper-raleigh scattering, Koen J. Clays, Rita
            Vos, Andre Pierre Persoons, Katholieke Univ.
            Leuven, Belgium...............................

PD3   Quadratic electro-optical measurements of
            polythiophene films by a modified mach-zehnder
            interferometer, C. Jakobsen, Jan Conrad
            Petersen, T. Geisler, Thomas Bjornholm, Daniel
            R. Greve, R. M. McCullough, Danish Inst. of
            Fund. Metrol., Denmark........................

ORAL SESSION, September 12, 1995, Holladay Room

PD4   Third harmonic dispersion studies of centrosymmetric
10:45am-   and noncentrosymmetric squaraines, James H. Andrews,
11:00am   John D.V. Khaydarov, Kenneth D. Singer, Diana L. Hull,
            Kathy C. Chuang, Case Western Reserve Univ., USA......

ORAL SESSION, September 13, 1995, Holladay Room

PD5   Efficiency of photoassisted poling of azobenzene,
2:30pm-   stilbene and biphenyl dyes as studied by stark
2:45pm   spectroscopy, Woltgang O. Haase, S. Grossmann, T.
            Weyrauch, L. M. Blinov, Technical Univ.
            Darmstadt, USA................................

PD6   Coherent detection of freely propagating
2:45pm-   terahertz radiation by electro-optic sampling in
3:00pm   a poled polymer, Ajay Nahata, Tony F. Heinz,
            David H. Auston, Chengjiu Wu, Columbia Univ.,
            USA...

PD7   Real and imaginary components of the third-order
5:45pm-   nonlinearity of polyaniline dodecylbenzenesulfonic
6:00pm   salt, Anna Samoc, Marek Samoc, Barry Luther-Davies,
            J. Swiatkiewicz, C. Q. Jin, J. W. White, Australian
            National Univ., Australia.....................

OSA Annual Meeting, 1995
Portland, OR.
Organic Thin Films '95 Topical Meeting

Organic Thin Films on the 30-kJ OMEGA Glass Laser System

A. Schmid, T. Kessler, K. Marshall, and J. Armstrong
Laboratory for Laser Energetics, University of Rochester
250 East River Road
Rochester, N.Y. 14623-1299

Abstract

Passive, organic thin films perform key optical-phase-control functions on the new, 30-kJ (351-nm) OMEGA glass laser system. Thin-film control-device performance requirements, material selection criteria,and in-system use experiences are reported. Performance limits and next-generation device requirements will be discussed as well.

Organic Thin Films on the 30-kJ OMEGA Glass Laser System

A. Schmid, T. Kessler, K. Marshall, and J. Armstrong
Laboraotry for Laser Energetics, University of Rochester
250 East River Road
Rochester, N.Y. 14623-1299
E-mail: asch@ftp.lle.rochester.edu

Laser-driven Inertial Confinement Fusion (ICF) increasingly depends on time-averaged on-target beam-smoothing methods for enhanced implosion uniformity in spherical targets. This is particularly true for the "direct-drive" approach in which multiple, symmetrically arranged UV laser pulses create an outward-streaming plasma which, by momentum conservation, causes the target shell to accelerate inwards and thereby increase fuel pressure and temperature to the point of nuclear ignition. Organic thin films play pivotal roles in phase control and beam smoothing of all 60 beams of the University of Rochester OMEGA laser, the currently most powerful UV laser for fusion development in existence.

In accordance with fusion-scale lasers' staged design and the concommittant separation of the OMEGA system into IR and UV sections (separated by the KDP frequency-tripling crystals), organic thin films find passive-device use in both the IR and UV system portions of OMEGA. In the following, they will be described sequentially.

1053-nm organic materials and phase corrector devices

Oveall beam focusabilitydrives the need for minimum phase errors on pulses propagating through OMEGA's multiple glass-amplifier stages. In spite of vigorous efforts by component manufacturers and a most stringent system-integration error budget, upon completion of system assembly each beam line exhibits considerable, cumulative, static phase error (as opposed to dynamic phase error due to air turbulence and optical nonlinearities turned on during pulse propagation). In order to compensate for this static phase error individually, each beam line can be equipped with its own, spatial phase corrector.

The phase corrector is placed early in each beam line at a low-fluence point, with the objective of introducing conjugate phase errors that exactly cancel the static error characteristic for this beam line. As the static error is not necessarily circularly symmetric, the corrector needs to be made from materials and by methods that are not circularly restrictive, i.e. other than conventional polishing methods. Photolithography offered greatest advantages from a process-integration viewpoint: the phase error is calculated from a 2-D interferogram generated by a 1053-nm, cw, alignment beam, a conjugate map is calculated, taking into account known process nonlinearities, this map

is translated into a UV-exposure mask, a photopolymer spun onto a glass substrate is exposed through the mask, and, after exposure, is conventionally developed. The photopolymer *is* the IR phase-corrector material. By virtue of the high pixel resolution of both the 2-D image and the mask, as well as the 4 K gray-scale levels used in the 12-bit calculations, these correctors are not binary diffractive or multiple-step $\pi/2$ diffractive elements but *continuous-tone gray-scale elements* limited only by the specific characteristics of the photographic emulsion used in producing the optics.

Screening various photoresists for high-peak-power, IR-laser compatibility found Shipley STR1045 to be the material of choice. This conventional novolac/diazonaphthaquinone system is viscosity-adjusted by varying the solvent 1,2-propanediol monomethyl ether acetate to yield up to 10-μm thick, interferometrically uniform films. With proper filtration against extrinsic particulate contamination and with all material-handling and device-preparation operations carried out in a clean room, 1053-nm laser damage is introduced into this polymer only at fluences exceeding 5 J/cm^2 (@ 1 ns pulse length).

Distributed phase plates and 351-nm organic materials

Photolithographically generated phase correctors are also at the core of 351-nm distributed phase plates. These phase elements are placed at the end of each UV beam line, immediately ahead of the target-focussing lens and the vacuum window.

Distributed phase plates (DPP's) help smoothen the UV-beam irradiance on target. Owing to turbulence and other, lesser effects, UV beams arriving on target exhibit significant speckle deviating from the smooth, spatial intensity envelope considered theoretically for each beam. For the purpose of excerting control over this speckle, DPPs aim at transforming the incident speckle-size distribution into a new distribution peaked at higher spatial frequencies, in essence making the speckle worse at first. However, this disadvantage is turned to advantage by electro-optically color cycling the beam in a manner that spatially blue- and red-shifts, so far in only one dimension, edges of each beam relative to its center. By modulating the 1-ns laser pulse between 1 and 10 Ghz, this color spread across the beam flips colors between 1 and 10 times over the length of the pulse. The interference effects between various spatial segments of the beam on target therefore vary with instantaneous color condition at the DPP, making fine speckle disappear at one location and reappear at another . This constitutes *time-integrated smoothing*.

For DPPs to deliver beams in form of high-frequency speckle on target without diffractive energy losses into non-target areas, DPPs also embody continuous-tone surface-relief features. Their use in the 4 J/cm^2, UV section of OMEGA prevents use of photoresist polymers as phase-control material. Additional materials and processing methods are needed for implementation of these devices at 31-cm clear-aperture size.

The following parameters guided materials design and development.

- UV laser-damage threshold: not lower than 4 J/cm^2.
- room-temperature miscibility of monomers, if a thermoset is used
- compatibility with applying AR layer by sol-gel technique
- ease of polymer removal and substrate recovery in case of fabrication error, handling damage or laser damage
- environmental stability under normal laboratory conditions
- mild synthesis conditions, low toxicity, no decomissioning problems.

Two technologies were explored for fabricating controlled surface-relief patterns. One approach to fabricating large-diameter, figured elements involves embossing a thermo-plastic by a metal master derived from a photolithographically prepared surface. The critical element is the metal stamper's durability, reliability and manufacturing cost. For these reasons combined, embossing of DPP surface structures was *not deemed useful*.
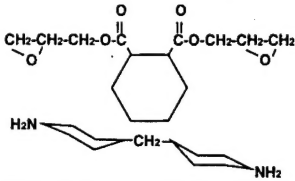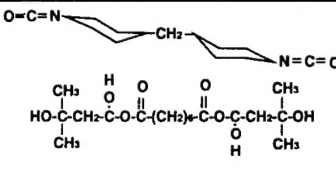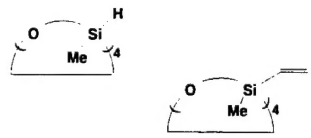
The approach chosen is condensation-reaction molding of thermoset monomers within the gap space between a flat fused-silica substrate and a photoresist master equipped with a release-medium top layer, of a composition other than the photoresist itself. The monomer fluid mixture is kept confined for the time required to completely crosslink. Depending on the polymer, this crosslinking may be carried out at room temperature or at elevated temperature $< T_g$ (photoresist) - 30° K, i.e. < 90° C. This scheme rules out condensation systems yielding gaseous reaction byproducts or requiring solvents, as either one may attack the release medium or cause entrapment and/or bubble formation and subsequent light scattering losses. Furthermore, the crosslinking rate must be such that the final product's bulk homogeneity remains uniform while allowing for alignment adjustments during production to be made without haste between the DPP substrate and the photoresist master element, both being masses of the order of 15 kg.

Several polymer systems were found to meet our requirements, although, at the time a process committment had to be made, one system was clearly superior. They are an aliphatic epoxide, an aliphatic urethane, and a catalyzed cyclo-siloxane glass. For the current generation of DPPs on OMEGA the aliphatic epoxide is used. The monomer structures, glass-transition temperatures and UV laser-damage thresholds for all three materials are listed in Table I. All three materials are used neat and none attacks the release medium.

The key advantages of the *aliphatic epoxide* are the clean, commercially available starting monomers requiring only particulate removal by filtration for adequate laser-damage resistance and the preferred viscosity of the degassed monomer mixture at room temperature for fabrication purposes. The major disadvantage is the added care needed in oxidation prevention of both the limited-shelf-life diamine and of the mixture during cure: all mixing and assembly operations must be carried out in a nitrogen-filled glove box.

Since in our replication process time is not of essence, a 24-hour crosslinking time before separation from the master is acceptable.

Table 1.   Polymers and their Characteristics

Monomers	Cat?	Tcure	Tg	UV Damage Threshold
	No	RT 24h	56C	1-on-1: 4.41 J/cm^2
				N-on-1: >6.5 J/cm^2
	No	80C 24h	88C	1-on-1: 3.28 J/cm^2 [*]
				N-on-1: 5.56 J/cm^2 [*]
	Wilkinson	80C 24-48h [**]	>250C , if any	1-on-1: 3.96 J/cm^2 [**]
				N-on-1: 4.12 J/cm^2 [**]

*   *after removal of trace amounts of BHT*
**   *depending on residual catalyst left after treatment by activated charcoal, ultracentrifugation and 0.45 μ m membrane filtration*

The *aliphatic urethane* does not require operations to be carried out under a nitrogen blanket, but it does need elevated-temperature cure for adequate crosslinking. For UV laser-damage thresholds to remain above 4 J/cm^2, the commercially available diisocyanate must be freed from traces of BHT. More significantly, the degassed monomer mixture shows much lower, room-temperature viscosity and, thereby, makes fabrication operations more difficult.

In order to provide greatest manufacturing flexibility, the third candidate material, the *catalyst-promoted cyclosiloxane glass,* was introduced. By stopping the polymerization (hydrosilylation) reaction through catalyst removal (the Wilkinson catalyst is used in polymer-supported form, 20-60 mesh) at the moment when the mixture viscosity is optimum for processing, a prepolymer with good, room-temperature shelf life is created that relieves manufacturing of mixing and degassing operations. However, depending on the residual amount of catalyst left, the cure time to completion varies, and, more important, the UV laser-damage threshold drops with increasing catalyst density. In its current composition, the glassy polymer also tends to be too brittle for existing release mechanisms from the photoresist master. Substituting some linear, allyl-endcapped siloxanes as "plastisizers", appears as promising modification to the current formulation.

Suppression of multi-photon fluorescence in hyper-Rayleigh scattering

Koen Clays, Rita Vos, and André Persoons

Laboratory of Chemical and Biological Dynamics,
Center for Research in Molecular Electronics and Photonics,
Department of Chemistry, University of Leuven,
Celestijnenlaan 200D, B-3001 Leuven, Belgium

Tel.: +32/16/32.75.08
Fax.: +32/16/32.79.82

ABSTRACT

We propose the suppression of the multi-photon fluorescence contribution to the hyper-Rayleigh scattering signal at the second-harmonic wavelength by phase-sensitive detection.

Suppression of multi-photon fluorescence in hyper-Rayleigh scattering

Koen Clays, Rita Vos, and André Persoons

Laboratory of Chemical and Biological Dynamics,

Center for Research in Molecular Electronics and Photonics,

Department of Chemistry, University of Leuven,

Celestijnenlaan 200D, B-3001 Leuven, Belgium

Tel.: +32/16/32.75.08

Fax.: +32/16/32.79.82

SUMMARY

The development of hyper-Rayleigh scattering (HRS) as an experimental technique for the determination of the first hyperpolarizability of molecules in an isotropic solution was based on the generic Q-switched Nd^{3+}:YAG laser type.[1] We have recently demonstrated that it is possible to replace this low repetition rate, nanosecond pulse laser source by a tunable, continuous-wave femtosecond system. This new system is based on the self-modelocked Titanium-sapphire laser. The fast gated electronics that are needed with the low duty-cycle of nanosecond HRS[2] are replaced by phase-sensitive detection.[3]

Multi-photon fluorescence (MPF) can complicate HRS measurements, because of the overlap in wavelength space of the HRS and MPF signal. Although for two-photon fluorescence (2PF), the Stokes shift between excitation and emission could in principle be large enough to prevent spectral overlap, the intrinsically broad spectral content of an ultrashort pulse does result in overlap of HRS and 2PF. Anti-Stokes two-photon fluorescence, also known as "hot fluorescence", has been reported to overlap with the HRS signal.[4,5] For three-photon fluorescence (3PF), it is possible that the emission spectrum extends from the third-harmonic over the second-harmonic wavelength. Spectral discrimination is, hence, not a generally applicable approach to separate HRS and MPF to the second-order nonlinear optical response. Because of the typical fluorescence lifetime of nanoseconds, the pulses with a duration of 10 nsec from a Q-switched YAG laser cannot be used for temporal discrimination between HRS and MPF. We demonstrate the possibility to discriminate by applying the recently demonstrated femtosecond HRS and phase-sensitive modulation techniques.

The molecule with second-order nonlinear optical (NLO) properties that was chosen for this study is 4-[2-(N,N-methyl,octadecyl-4-aminophenyl)-ethenyl]-N-methyl-pyridinium bromide (see Fig. 1). This is an ionic molecule that has been designed for incorporation in Langmuir-Blodgett (LB) films. It is complementary to the 4-[2-(N,N-dimethyl-4-amino-phenyl)-ethenyl]-N-docosyl-pyridinium bromide.[6] Stable Y-type deposition of alternating

layers from these two NLO chromophores results in a non-centrosymmetric LB film. The first hyperpolarizability from these molecules can not be measured by Electric-Field-Induced Second-Harmonic Generation (EFISHG) since no orienting dc field can be applied over the solutions. The first hyperpolarizability has been deduced from coherent frequency-doubling in LB films. This value proved to be a sensitive function of LB substrate preparation, deposition conditions, and concentration, with a maximum value of 1200 x 10^{-30} esu at 1.064 µm.[7] A direct determination of the first hyperpolarizability in solution would eliminate these influences, but multi-photon fluorescence has complicated the HRS measurements so far.
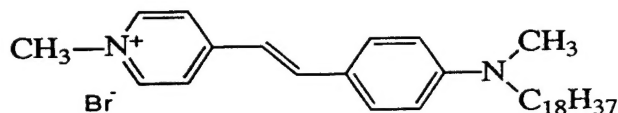
Fig. 1. Molecular structure of NLO dye used.

The molecule was dissolved in CHCl$_3$ at a concentration of 10^{-2} M. The cut-off wavelength for (linear) absorption is 600 nm. Narrow-band low power excitation at 600 nm in a spectrofluorimeter induces linear, one-photon fluorescence (1PF) with a maximum at 620 nm. Wide-band excitation at 1.2 µm from a femtosecond optical parametric oscillator (OPO) induces 2PF, together with the HRS signal. Figure 2 shows the relative contributions of HRS and 2PF to the observed second-order signal. This signal was collected with a monochromator with 4 nm resolution. The spectral width of the HRS peak is determined by the convolution of this resolution with the spectral width of the 80 femtosecond pulse. The 2PF contribution (solid line in Fig. 2) should be convoluted with the intrinsic width of the exciting femtosecond pulse. From Fig. 2, it is clear that, due to the spectral width of the femtosecond pulse, there is intrinsic overlap of HRS with 2PF. This overlap can be much worse when anti-Stokes 2PF is observed, or in the case of 3PF.

Two approaches are possible to discriminate between the HRS and the MPF contributions. Directly in the time domain, gated integrators could be used with their gate window appropriately set to exclude the time-delayed fluorescence. Gated integrators can not be used at the high repetition rate of mode-locked lasers (80 MHz). Lowering this rate with a pulse-picker would significantly reduce the signal-to-noise ratio of the measurement. Because of the high repetition rate, modulation techniques with phase-sensitive detection are applicable.[3] Such modulation (cross-correlation) techniques have been developed specifically for the measurement of the fluorescence lifetimes of fluorophores through the phase-shift between immediate (linear) scattering and the delayed fluorescence.[8-10] The same principle can be applied to discriminate between HRS and 2PF. Phase-sensitive detection[11] in quadrature with the phase-shifted 2PF component results in the detection of the HRS component without the fluorescence. Figure 3 shows the amplitude of the cross-correlation signal and the relative phase of the signal as a function of wavelength. The modulation

harmonic (240 MHz) of the fundamental repetition rate. It is clear that a difference in phase can be observed between the HRS contribution (to the left of Fig. 3) and the 2PF (to the right of Fig. 3).
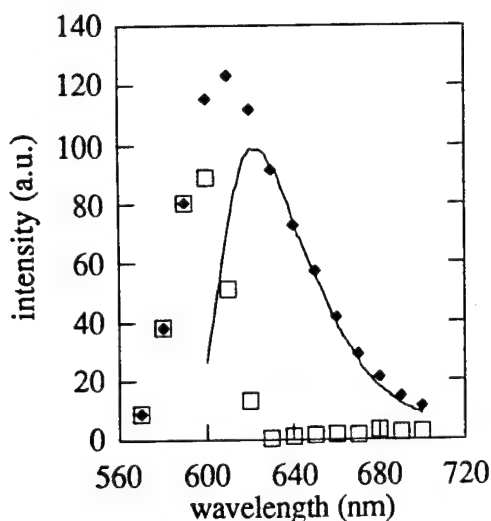
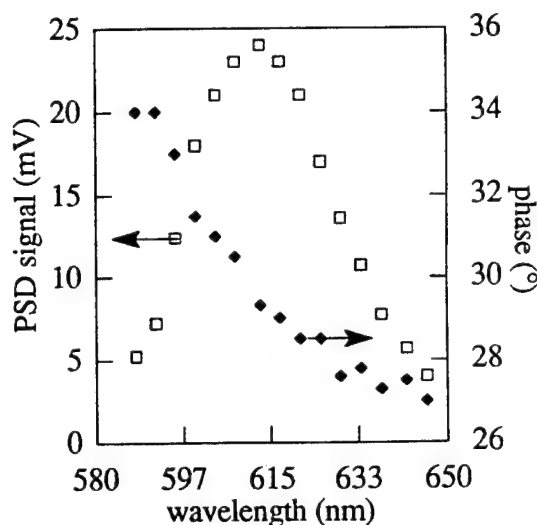Fig. 2. Relative contributions of 2PF (solid line) and HRS (squares) to the second-order signal (crosses).

Fig. 3. Amplitude and phase of the cross-correlation signal

The fluorescence decay of the solution has been measured by multi-frequency phasefluorometry. For this measurement, the (narrow-band) excitation was at 600 nm. The phase shift ϕ between scattering and fluorescence was measured at a set of 50 modulation frequencies between 0.4 and 900 MHz and for wavelengths from 610 to 650 nm. Fig. 4 shows the data and the graphical evaluation of the data reduction for emission at 610 nm.
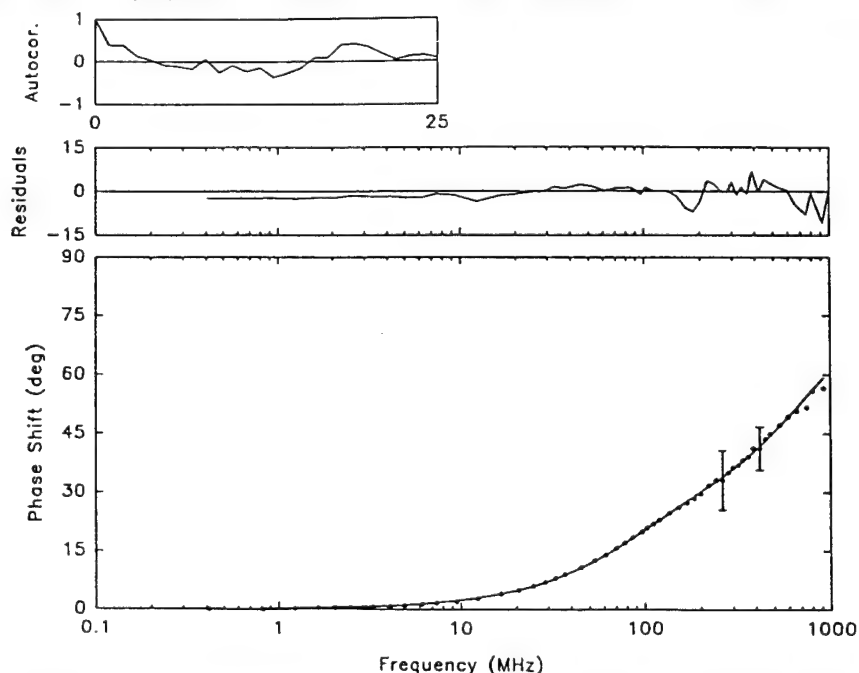
Fig. 4. Phase shifts and graphical evaluation for a fit to a bi-exponential fluorescence decay for 10^{-2} M of NLO dye (see Fig. 1) in CHCl$_3$

The fluorescence decay is double-exponential with two short lifetimes (0.3 and 1.3 nsec). The multi-wavelength analysis shows that there is variation of the lifetimes and their contribution, as evidenced by different phase shifts, at wavelengths where there is clearly only fluorescence and no (linear) scattering. The numerical quality parameters of the fit (*e.g.* the reduced chi-square) and the graphical evaluation indicate that a simple (bi-exponential) decay is not a complete description. The rather short fluorescence lifetimes are indicative of excited-state reactions. The high concentration of the chromophore makes this very likely.

The complex (not single exponential) decay of the fluorescence is a problem for phase-sensitive detection in quadrature, because the phase ϕ changes with wavelength, and most likely also with concentration. The relatively small value of the phase shift ϕ (due to the short lifetimes) is also a problem, since the complete suppression of the 2PF component also reduces the HRS component by sin ϕ. A 90° phase shift would not affect the HRS at all. This value of the phase shift is the limit for high modulation frequencies. For high frequencies, the demodulation of the fluorescence is also complete. In other words, the ac component of the fluorescence has disappeared and only a dc component is left. However, at high modulation frequencies, the phase noise of the laser becomes increasingly important in phase-sensitive detection.[12] Especially with free-running self-modelocking, as used in Titanium-sapphire lasers, the phase noise is extremely large. It is proposed to use a cavity-length stabilized femtosecond laser in conjunction with a sensitive detector with high bandwidth (microchannel plate detector, 2 GHz). Modulation at this frequency would cause a very large phase shift between scattering and fluorescence, or, equivalently, almost complete demodulation of the fluorescence. The only ac component the fast detector would be able to pick up at this high frequency would be the hyper-Rayleigh scattering. In this way, the contribution coming from fluorescence, be it two-photon-, three-photon- or anti-Stokes two-photon fluorescence, would be completely suppressed. Measurement of the HRS ac amplitude versus fundamental intensity and versus concentration - the well-known procedure for HRS - would then enable the direct, experimental determination of the first hyperpolarizability of fluorescent compounds.

(Measurements of the phase-shift (life-times) as a function of concentration are under way. The installation of the cavity-length stabilized system is scheduled for the end of this year. Actual hyperpolarizability measurements have to await this phase stability.)

1. K. Clays and A. Persoons, *Phys. Rev. Lett.* **66**, 2980 (1991).
2. K. Clays and A. Persoons, *Rev. Sci. Instrum.* **63**, 3285 (1992).
3. K. Clays and A. Persoons, *Rev. Sci. Instrum.* **65**, 2190 (1994).
4. M.C. Flipse, R.d. Jonge, A.W. Marsman, C.A.v. Walree and L.W. Jenneskens, *Organic Thin Films for Photonic Applications, 1995, paper ThA2* (1995).
5. C. Dhenaut, I. Ledoux, I.D.W. Samuel, J. Zyss, M. Bourgault and H.L. Bozec, *Nature* **374**, 339 (1995).
6. J.S. Schildkraut, T.L. Penner, C.S. Willand and A. Ulman, *Opt. Lett.* **13**, 134 (1988).
7. P. Winant, Ph.D. thesis, University of Leuven, Belgium (1990).
8. J.R. Lakowicz, G. Laczko and I. Gryczynski, *Rev. Sci. Instrum.* **57**, 2499 (1986).
9. K. Clays, J. Jannes, Y. Engelborghs and A. Persoons, *J. Phys.E: Sci. Instrum.* **22**, 297 (1989).
10. R. Vos, Y. Engelborghs, J. Izard and D. Baty, *Biochemistry* **34**, 1734 (1995).
11. S.M. Keating-Nakamoto, H. Cherek and J.R. Lakowicz, *Anal. Chem.* **59**, 271 (1987).
12. K. Clays and A. Persoons, *Appl. Opt.* **27**, 3601 (1988).

Quadratic Electro-optical Measurements of Polythiophene Films by a Modified Mach-Zehnder Interferometer.

We report the measurement of quadratic electro-optical coefficients of head-to-tail poly(3-dodecylthiophene) using a modified Mach-Zehnder interferometer at 633 nm. We find $s_{1133} = 3.7 \times 10^{-20}$ m²/V² and $s_{3333} = 4.1 \times 10^{-20}$ m²/V².

C.Jakobsen[1], J.C.Petersen[1], T.Geisler[2], T.Bjørnholm[3], D.R.Greve[3], and R.M.McCullough[4].

[1] Danish Institute of Fundamental Metrology, Anker Engelundsvej 1, Bld.307, DK-2800 Lyngby, Phone: +45 4593 1144, Fax: +45 4593 1137,

[2] Institute of Physics, Aalborg University, Pontoppidanstræde 103, DK-9220 Aalborg

[3] CISMI, Chemistry Department, University of Copenhagen, Fruebjergvej 3, DK-2100 Copenhagen.

[4] Chemistry Department, Carnegie Mellon University, Pittsburg, USA.

Quadratic Electro-optical Measurements of Polythiophene Films by a Modified Mach-Zehnder Interferometer.

C.Jakobsen[1], J.C.Petersen[1], T.Geisler[2], T.Bjørnholm[3], D.R.Greve[3], and R.M.McCullough[4]

[1] *Danish Institute of Fundamental Metrology, Anker Engelundsvej 1, Bld.307, DK-2800 Lyngby, Phone: +45 4593 9344, Fax: +45 4593 1137,* [2] *Institute of Physics, Aalborg University, Pontoppidanstræde 103, DK-9220 Aalborg,*
[3] *CISMI, Chemistry Department, University of Copenhagen, Fruebjergvej 3, DK-2100 Copenhagen,* [4] *Chemistry Department, Carnegie Mellon University, Pittsburg, USA.*

There are still many unanswered questions with respect to which parameters in the molecular structure that are important in the nonlinear optical interaction. Therefore, a need for new and improved experimental methods for measuring the nonlinear coefficients of molecular materials with potential for nonlinear optics still exists.

Here, the quadratic electro-optical coefficients of head-to-tail (HT) poly(3-dodecylthiophene) (see Figure 1) are measured by use of a modified Mach-Zehnder interferometer at 633 nm. The setup allows for measurement of both the real imaginary parts of the quadratic electro-optical coefficients s_{1133} and s_{3333}. This modified arrangement has the advantage that a more reliable film thickness is obtainable. For comparison with other experiments we have studied 2-methyl-4-nitroaniline (MNA) and Disperse Red (DR1) dissolved in a PMMA matrix. We compare our results with previously reported ones.

Experimental Method and Setup.

The most common methods used for determining the quadratic electro-optical coefficients s_{1133} and s_{3333} are the ellipsometric and interferometric methods. In ellipsometry, only the difference between the two quadratic electro-optical coefficients is determined and thus no absolute values are obtained [3]. In interferometric methods the absolute value of the two coefficients can in principle be determined. However, in the literature some authors using ellipsometry also determine absolute values by assuming a ratio of the two coefficients of 3 [3,4,5]. It has been pointed out that this is valid only in the case when the quadratic electro-optical response is purely electronic [6,7]. In fact, the signal may be composed of other than the electronic contribution: e.g. electrostriction, electrode attraction and reorientational contribution. In Mach-Zehnder, or Michelson interferometry the polymer film is usually sandwiched between two ITO glass substrates. In such an arrangement it is difficult to verify the resulting film thickness.

In the present work we use another sample geometry for a slightly modified Mach-Zehnder interferometer which also allows for ellipsometric measurements on the same sample (see Figure 2). The setup has previously been suggested by Norwood et al. [8] for measuring linear electro-optical coefficients.

In this work the polymer film is formed on an ITO coated glass slide by dip coating. A layer of aluminium is then deposited on the polymer film by evaporation and an electric field can be applied across the polymer film perpendicular to the film plane. The thickness of the polymer film is determined either from the absorption spectrum or from the Fabry-Perot effect observed in the absorption spectrum. The sample is used as one of the mirrors of the Mach-Zehnder interferometer (see Figure 2).

With s-polarized light s_{1133} can be obtained. First, the contrast of the interference pattern in the plane of the detector is measured. Then the quasistatic electric field is applied to the sample (a few kHz) and the quadratic electro-optical signal is measured at twice the modulation frequency of the electric field while the phase difference between the two beams is changed by translating the wedge. This is shown in Figure

2a and 2b, respectively. With p-polarized light the same operation is carried out and s_{3333} can be obtained. The coefficients s_{1133} and s_{3333} are easily determined from the following expression:

$$s_{ii33,R} = \frac{Re\{n_0^3 s_{ii33}\}(n_{0R}^3 - 3n_{0R}n_{0I}^2) - Im\{n_0^3 s_{ii33}\}(n_{0I}^3 - 3n_{0I}n_{0R}^2)}{n_{0I}^6 + n_{0R}^6 + 3n_{0I}^2 n_{0R}^4 + 3n_{0R}^2 n_{0I}^4}$$

$$s_{ii33,I} = \frac{Im\{n_0^3 s_{ii33}\}}{(n_{0R}^3 - 3n_{0R}n_{0I}^2)} + s_{ii33,R}\frac{(n_{0I}^3 - 3n_{0I}n_{0R}^2)}{(n_{0R}^3 - 3n_{0R}n_{0I}^2)}$$

(1)

where $i=1,3$, the real and imaginary parts of $(n_0^3 s_{ii33})$ are measured values [9], $s_{ii33} = s_{ii33,R} + i\, s_{ii33,I}$ and $n_0 = n_{0R} + i\, n_{0I}$, with n_{0R} and n_{0I} being the real and imaginary parts of the linear refractive index.

If the linear absorption is negligible ($n_{0I}=0$) Eq.(1) becomes much simpler. For comparison the sample can also be investigated by ellipsometry, since the setup is easily modified to an ellipsometer probing exactly the same position on the sample as the Mach-Zehnder interferometer.

Measurement.

Reference film samples of DR1 and MNA dispersed in poly-(methyl-metacrylate) (PMMA) were made. For both compounds the compound-to-PMMA ratio was 10% by weight and the film thicknesses were in the range of 1 micron to 4 microns.

Both molecules contain a π conjugated electron system, which has been shown to be of significant importance for optical third order nonlinearities [2].

For MNA we find $s_{1133}=(3.0+i0.1)\times10^{-21} \pm 20\%$ m²/V² and $s_{3333} = (4.1+i0.5)\times10^{-21} \pm 30\%$ m²/V². The ratio s_{3333}/s_{1133} of $1.4 \pm 40\%$ and for DR1 $s_{1133}=(5.6+i0.1)\times10^{-21} \pm 25\%$ m²/V² and $s_{3333} =(1.1+i0.1)\times10^{-20} \pm 20\%$ m²/V² with a ratio s_{3333}/s_{1133} of $1.9 \pm 20\%$.

The modest imaginary part of s_{ii33} for the two types of film is due to an off-resonance probe beam.

The origin of the QEO effect has not been investigated, therefore, more studies are needed. Though, the contribution from electrostriction and electrode attraction was proven to be negligible by measurements on an undoped PMMA film. It can be shown that if the signal origins purely from molecular reorientation in the DC-field the ratio of s_{3333}/s_{1133} is -2, and if the signal origins purely from the electronic response it is 3 [10]. Thus it it most likely that the QEO effect origins from a mixture of (at least) these two sources at 633 nm.

Other authors have reported on quadratic electro-optical measurements of MNA and DR1. Kumar et al. [11] repport an s_{1133} at 633 nm of almost an order of magnitude smaller than the value found here. They are using a Mach-Zehnder interferometer which measures only s_{1133}. There is no obvious reason for the large difference between their and our measurements from the information available in their paper. Ono et al. [12] and Kuzyk et al. [13] report on quadratic electro-optical measurements of DR1 in PMMA and determine s_{1133} to be a factor of 3 and 4, respectively, smaller than the one we report here. Again, there is no obvious reason for the difference. However, it is of importance to resolve this issue.

The polythiophene films were prepared as described for the reference films. The polythiophene is almost 100% HT. The polythiophene molecules are microscopically preferentially oriented in the plane of the film [14]. Therefore, we do not expect the film to be isotropic in either the linear or nonlinear optical response. This means e.g. that s_{3333} is not equal to s_{1111}. Because of the sample geometry in the experimental setup we are restricted to measure only s_{1133} and s_{3333}. In this preliminary study we will assume the linear refractive index to be isotropic, for simplicity, and we find $s_{1133}=3.7\times10^{-20}$ m²/V² and

$s_{3333} = 4.1 \times 10^{-20}$ m^2/V^2. The imaginary part of s_{1133} is about one order of magnitude smaller than the real part and for s_{3333} while the imaginary part is about one fourth of the real part. The ratio between the two coefficients suggests that there are other than electronic contributions to the signal. These coefficients are not large compared to the reference materials. However, it should be noted that the DC-field is applied perpendicularly to the film plane, i.e. perpendicular to the highly mobile conjugated electronic system. An obvious experiment would be to redesign the sample geometry so the DC-field can be applied in the direction of the conjugated electronic system of the Polythiophene.

Conclusion.

We have measured quadratic electro-optical coefficients of two reference materials and HT Poly(3-dodecylthiophene) films. The coefficients of the Polythiophene are absolutely measureable without being uniquely high. Though, when considering that the polymer chains are in the plane of the film and the DC-field is applied perpendicular to this plane we expect a much higher s_{1111} (in-plane) than s_{3333}. We suggest that the Polythiophene should be measured for another sample geometry which allows the DC-field to be applied in the plane of the film.
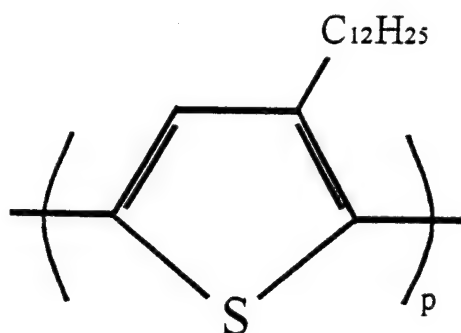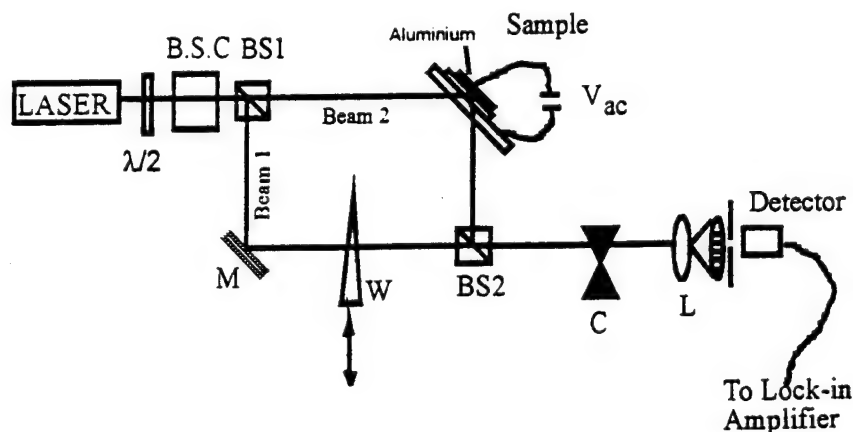

Figure 1: Poly(3-dodecylthiophene).

Figure 2: Modified Mach-Zehnder interferometer. BSC is a Babinet-Soleil Compensator, M a mirror, W a wedge, λ/2 a halfwave plate, BS1 and BS2 beamsplitters, C a chopper and L a lens.
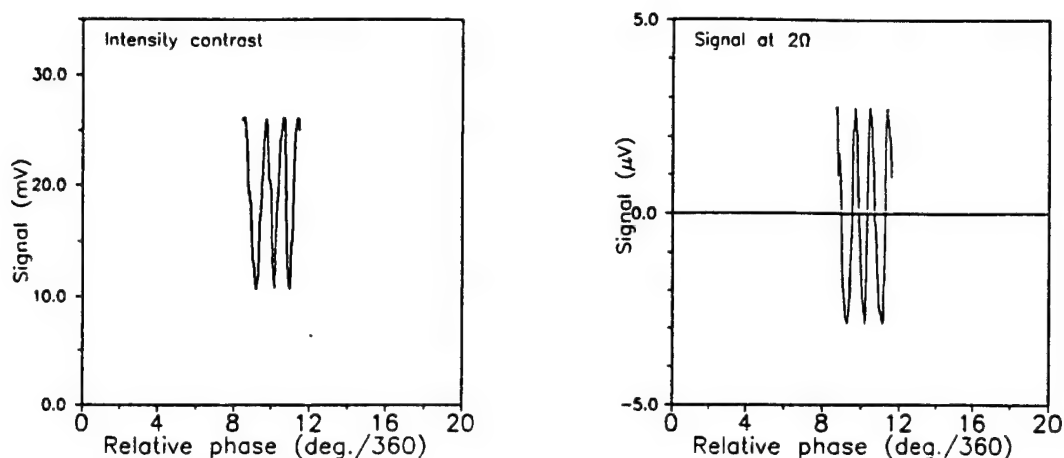
Figure 3: Measurement of a) the intensity of the interference pattern and b) the quadratic electro-optical signal as function of the phase difference.

[1]   L.S.Pu in "Materials for Nonlinear optics" - Chemical Perspectives, S.R.Marder et al., eds., ACS Symposium Series **455**, 331 (1991).
[2]   "Molecular Nonlinear Optics", Academic Press (1994), Ed.J.Zyss.
[3]   Y.Lévy, P.A.Chollet, G.Gadret, and F.Kajzar, SPIE vol.1775, 299-310, Nonlinear Optical Properties of Organic Materials V (1992).
[4]   Y.Lévy, M.Dumont, E.Chastaing, P.Robin, P.A.Chollet, G.Gadret, and F.Kajzar, Mol.Cryst.Liq.Cryst.Sci.Technol.B: Nonlinear Optics, **4**, 1-19 (1993).
[5]   P.Röhl, B.Andress, and J.Nordmann, Appl.Phys.Lett.**5**, 273-275 (1991).
[6]   D.Morchère, P.-A.Chollet, W.Flemming, M.Jurich, B.A.Smith, and J.D.Swalen, J.Opt.Soc.Am.**B10**,1894-1900 (1993).
[7]   C.Poga, T.M.Brown, M.G.Kuzyk, and C.W.Dirk, J.Opt.Soc.Am.**B12**,531-543 (1995).
[8]   R.A.Norwood, M.G.Kuzyk, and R.A.Keosian, J.Appl.Phys.**75**, 186-1874 (1994).
[9]   M.G.Kuzyk and C.Poga in "Molecular Nonlinear optics" Academic Press, 299-337 (1994), Ed. J.Zyss.
[10]   C.Poga, M.G.Kuzyk, and C.W.Dirk, J.Opt.Soc.Am.**B11**,80-91 (1994).
[11]   J.Kumar, A.K.Jain, M.Cazeca, J.Ahn, R.S.Kumar, and S.K.Tripathy, SPIE vol.1147 Nonlinear Properties of Organic Materials II, 177-181 (1989).
[12]   H.Ono, K.Misawa, K.Minoshima, A.Ueki, and T.Kobayashi, J.Appl.Phys.**77**,435-440 (1995).
[13]   M.G.Kuzyk, J.E.Sohn, and C.W.Dirk, J.Opt.Soc.Am.**B7**,842-858 (1990).
[14]   D.R.Greve, Ph.D.Thesis, University of Copenhagen (1995).

Third Harmonic Dispersion Studies of Centrosymmetric and Noncentrosymmetric Squaraines

James H. Andrews, John D. V. Khaydarov, and Kenneth D. Singer

Case Western Reserve University
Department of Physics, Cleveland, OH 44106-7079

Diana L. Hull and Kathy C. Chuang

NASA Lewis Research Center, Cleveland, Ohio 44135-3191

Third harmonic dispersion was measured in centrosymmetric and noncentrosymmetric squaraine molecular solutions. A large contribution to the third order nonlinearity from the 1Bu to 2Ag state was revealed. Contributions from ground and excited state dipole moments in ostensibly centrosymmetric and noncentrosymmetric dyes were observed.

Third Harmonic Dispersion Studies of Centrosymmetric and Noncentrosymmetric Squaraines

James H. Andrews, John D. V. Khaydarov, and Kenneth D. Singer

Case Western Reserve University
Department of Physics, Cleveland, OH 44106-7079

Diana L. Hull and Kathy C. Chuang

NASA Lewis Research Center, Cleveland, Ohio 44135-3191

Squaraine dyes have been the subject of recent studies due to their large and negative third-order optical nonlinearities.[1-5] In addition, it has recently been observed that highly symmetrical squaraine dyes can exhibit properties, such as optical second harmonic generation, normally associated with noncentrosymmetric materials. It has been concluded that polar isomers of these symmetrical dyes coexist with centrosymmetric species.[6] We describe here, experimental studies which reveal the important role of the lowest lying Ag state in the third order nonlinerity in the visible and near infrared. We also show evidence for the existance of polar isomers in these measurements of the spectral dispersion of third harmonic generation. We show how third harmonic spectral dispersion can directly probe the difference between the lowest excited and ground state dipole moments, a prime contributor to the second order optical nonlinearity, β. We have also studied this dipole moment difference in a noncentrosymmetric squaraine.

While the two-level model for β has been extensively used in the study of the response of organic dyes, relatively little research has focused on the relationship between β and the third order nonlinearity, γ, for noncentrosymmetric materials or on the limitations of the two-level model. The same molecular excited states contribute for both β and γ, but in different combinations and with different frequency dependence. The transition moments and dipole moment differences are the same in each case, though their relative importance depends on nonlinear process involved.

We have studied the lowest lying excited states, and the transitions between them using frequency dependent third harmonic generation. Of particular interest here are the results obtained for two centrosymmetric dyes, ISQ, and C16-ISQ, the ostensibly centrosymmetric squaraine dye, C16-ThSQ, and the noncentrosymmetric dye, C16-ISQ-BSQ, all structures pictured in Figure 1. We determined the transition moments between the lowest lying states of various symmetry by fitting the measured dispersion of γ in the vicinity of the $2A_g$ two-photon resonance to the simplified sum-over-states model with a minimum number of terms consistent with the linear absorption spectrum of the dyes studied and the observed third harmonic spectra.

To study the spectral dispersion of the third harmonic generated in low concentration solutions of the squaraine dyes, we used a synchronously pumped optical parametric oscillator (SPOPO) which produces tunable high power picosecond pulses

1

from 0.4-2.5 μm. Our SPOPO is pumped by the third harmonic (355 nm) of a pulsed Nd:YAG laser with a combination of hybrid active-passive mode-locking and passive negative feedback. To measure the third harmonic response in solution, we used a wedged liquid cell with thick (5 cm) input and output windows.
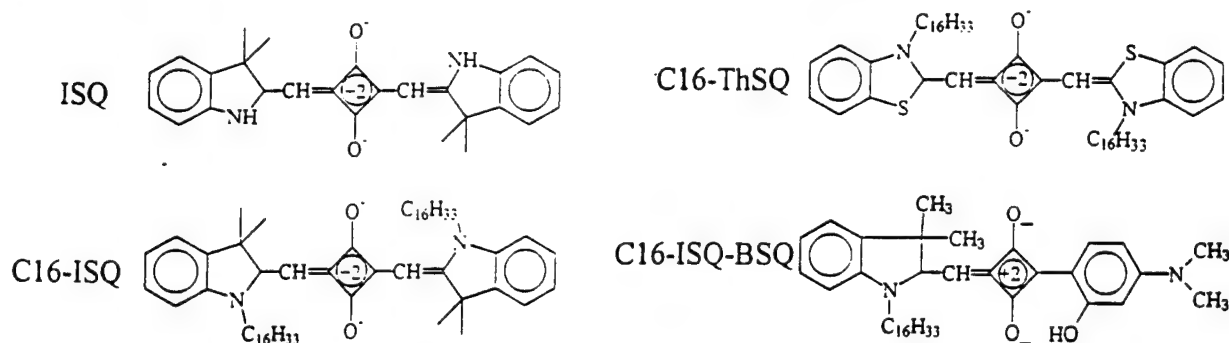

Figure 1. Molecular structure of the studied squaraines.

Figure 2 shows the experimentally determined intensity ratios for the specified concentrations of C16-ThSQ and C16-ISQ-BSQ in chloroform together with our least squares fits. The fit parameters for each dye are shown in Table 1.
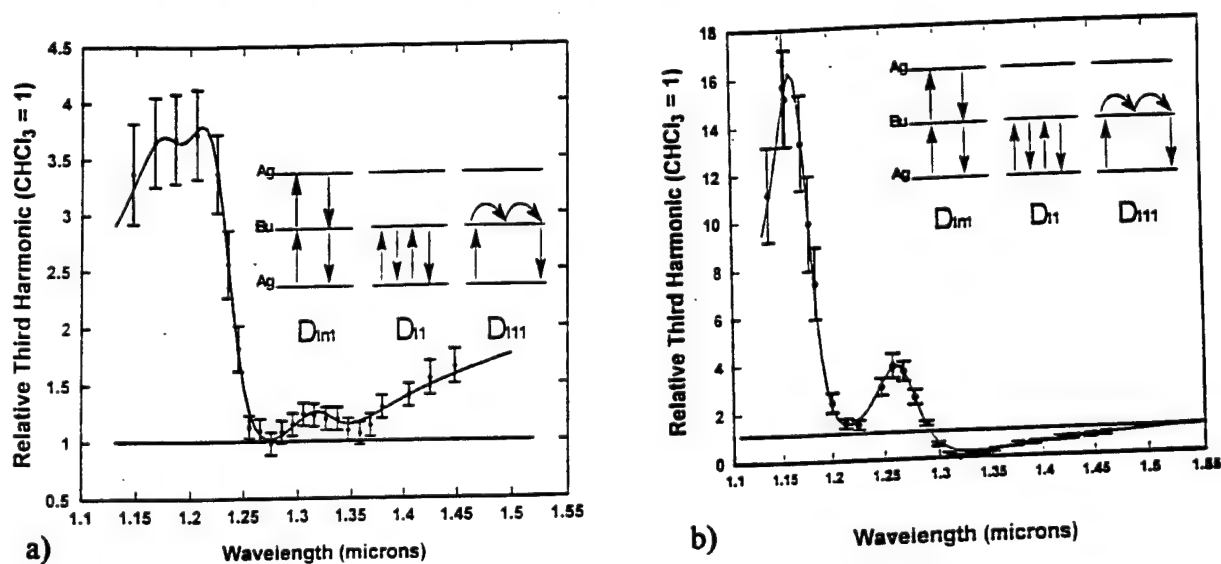

Figure 2. Third harmonic dispersion for a)C16-ThSQ and b)C16-ISQ-BSQ.

All of the dyes exhibit a major contribution from the 1Bu to 2Ag transition as well as from transitions from the 1Bu state to higher lying Ag states as deduced from our four state fits. From its structure, we would expect our results for C16-ThSQ to be similar to those for C16-ISQ and ISQ. To our surprise, however, a four-level model with "pure" two-photon levels was unable to account even qualitatively for an unmistakable secondary oscillation in the ratio of the third harmonic at around 1.3

2

to 1.4 μm fundamental. This resonance is consistent with the contribution of a term describing the difference between excited and ground state dipole moments.

Table 1. Fit parameters for dispersion of third harmonic generation.

ab levels	10	20	n0
ISQ ($\Delta\mu_{01} \equiv 0$)			
ω_{ab} (eV)	1.896 ± 0.004	2.05 ± 0.01	3.3 ± 1
Γ_{ab} (meV)	45 ± 3	33 ± 6	360 ± 120
μ (Debye)	$\mu_{01} = 10.3 \pm 1.4$	$\mu_{12} = 4.8 \pm 1$	$\mu_{1n} = 9.5 \pm 3$
C16-ISQ ($\Delta\mu_{01} \equiv 0$)			
ω_{ab} (eV)	1.95 ± 0.004	2.1 ± 0.01	5 ± 1.5
Γ_{ab} (meV)	33 ± 1	46 ± 9	370 ± 150
μ (Debye)	$\mu_{01} = 12.3 \pm 1.4$	$\mu_{12} = 6.0 \pm 1$	$\mu_{1n} = 12.2 \pm 3$
C16-ThSQ	($\Delta\mu_{01} = 1 \pm 0.5$ Debye)		
ω_{ab} (eV)	1.87 ± 0.006	2.02 ± 0.01	3.7 ± 1
Γ_{ab} (meV)	42 ± 3	50 ± 15	340 ± 120
μ (Debye)	$\mu_{01} = 11.8 \pm 1.4$	$\mu_{12} = 4 \pm 1$	$\mu_{1n} = 11 \pm 3$
C16-ISQ-BSQ	($\Delta\mu_{01} = 4 \pm 1.5$ Debye)		
ω_{ab} (eV)	1.95 ± 0.006	2.12 ± 0.01	4.5 ± 1.2
Γ_{ab} (meV)	40 ± 3	41 ± 15	300 ± 150
μ (Debye)	$\mu_{01} = 12.4 \pm 1.5$	$\mu_{12} = 6.2 \pm 1$	$\mu_{1n} = 11.7 \pm 3$

To test our interpretation of the results obtained for C16-ThSQ and to explore the possibility of using third harmonic spectral dispersion measurements to character-ize the ground-to-first-excited state dipole moment difference used for calculating β in noncentrosymmetric molecules, we then performed third-harmonic spectral mea-surements on C16-ISQ-BSQ. This molecule is clearly noncentrosymmetric though the donor end groups are not significantly different so that the broken symmetry is not expected to be as dramatic as in, for example, a push-pull polyene with a large in-trinsic dipole moment. As with C16-ThSQ, a four-level model is unable to account for the unmistakable additional peak in the ratio of the third harmonic between 1.2 and 1.3 μm fundamental. Due to the absence of absorption at the fundamental, the sum-over-states expression for the third harmonic requires that the feature be accounted for by an additional competing "resonance" near one-half (2ω) of the fun-damental wavelength for the oscillation. Since, the linear absorption peak for this

3

molecule is about 635 nm, this feature is located at the frequency appropriate to an intermediate transition between the ground state and the first excited state, which is only permitted for noncentrosymmetric systems. We fit the curve in Figure 2b to a four-level model with transition moments comparable to those of C16-ISQ except for the addition of a dipole moment difference of $\Delta\mu_{01} = 4$ Debye, which suggests a much stronger asymmetry than was seen in C16-ThSQ, as would be expected from its structure.

For C16-ThSQ, there are also features in the data below 1.2 μm that diverge from a model with just a single one-photon excited state. We believe these features, which may also be present to a lesser extent or at shorter wavelengths with ISQ, C16-ISQ, and C16-ISQ-BSQ, are due to the onset of a three-photon absorption in the near uv spectrum of the dye. We included a narrow ($\sim 70meV$) and weak, fifth level of odd parity ($\mu_{04} \sim \mu_{24} \sim 1$ Debye) around 390 nm in our fit for C16-ThSQ, consistent with the onset of the ultraviolet absorption band. The terms involving transitions between this higher-lying B_u state and the high-lying A_g states were ignored since they contributed no additional features in this wavelength region.

We conclude that the origin of the large negative third order nonlinearity in the visible and near infrared in squaraines can be explained through the competition between an extremely large negative contribution from the ground to 1Bu state, which is incompletely canceled by terms arising from transitions from that state to the 2Ag state and higher Ag states. We have observed strong evidence for noncentrosymmetric isomers of one squaraine dye, and have observed directly the dipole moment difference between the first excited and ground states in a noncentrosymmetric squaraine dye.

REFERENCES

1. C. W. Dirk and M. G. Kuzyk, "Squarilium dye-doped polymer systems as quadratic electrooptic materials," *Chem. Mat.* **2**, 4-6 (1990).
2. J.H. Andrews, J.D.V. Khaydarov, and K.D. Singer, "Contribution of the 2Ag State to the Third Order Optical Nonlinearity in a Squaraine Dye," *Opt. Lett.* **19**, 984-986, *errata* **19**, 1909, (1994).
3. Y. Z. Yu, R. F. Shi, A. F. Garito, and C. H. Grossman, "Origin of negative $\chi^{(3)}$ in squaraines: experimental observation of two-photon state," *Opt. Lett.* **19**, 786-788 (1994).
4. Q. L. Zhou, R. F. Shi, O. Zamani-Khamari, and A. F. Garito, "Negative third-order optical responses in squaraines," *Nonlinear Optics* **6**, 145-154 (1993).
5. J.H. Andrews, J.D.V. Khaydarov, K.D. Singer, D.L. Hull, and K.C. Chuang, "Spectral Dispersion of Third Harmonic Generation in Squaraines", *Nonlinear Optics* **10**, 227 (1995).
6. C.W. dirk, W.C. Herndon, F. Cervantes-Lee, H. Selnau, S. Martinez, P. Kalamegham, A. Tan, G. Campos, M. Velez, J.Zyss, I. Ledoux, and L.-T. Cheng, "Squarilium Dyes: Structural Factors Pertaining to the Negative Third-Order Nonlinear Optical Response,", it J. Am. Chem. Soc. **117**, 2214 (1995).

Efficiency of photoassisted poling of azobenzene, stilbene and biphenyl dyes as studied by Stark spectroscopy

W. Haase, S. Grossmann, S. Saal, T. Weyrauch, and L. M. Blinov[+]
Technische Hochschule Darmstadt, Institut für Physikalische Chemie,
Petersenstraße 20, 64287 Darmstadt, Germany
[+]permanent address: Institute of Crystallography, Russian Academy of Science,
Leninsky pr. 59, 117333 Moscow, Russia

Introduction

Besides the usual thermal assisted poling procedure the photoassisted poling reported for polymers containing azobenzene chromophores is of current interest. Usually the enhanced orientational mobility under illumination with visible light in the absorption band of the chromophore is explained by the trans⇔cis isomerization cycle of the azo dye, with a photoisomerization trans⇒cis and a thermal relaxation cis⇒trans. Because of the more compact shape of the cis isomer the rotational mobility is much higher than that of the trans isomer, thus polar orientation under electric DC field is possible. Since the memory of the polar orientation is lost only partially during the cis⇒trans transition, the trans isomers will achieve also a polar ordering [1-4]. This theory cannot be applied to systems containing stilbene dyes, where no thermal cis⇒trans relaxation is present. Investigations on systems containing stilbene dyes have also shown enhanced polar order in a poling process under illumination with visible light in the absorption range of the chromophore [5,6]. Thus the influence of heating of the sample (both macroscopically and microscopically in the vicinity of the dye molecule) must be discussed. The aim of this work is to compare the photoassisted poling behaviour of azo and stilbene dyes as well as of a non isomerizable biphenyl dye.

Stark spectroscopy

For the measurement of the poling efficiency, i. e. the degree of polarity of a poled sample, we used the Stark (or electroabsorption) spectroscopy technique [5,7]. Contrary to conventional methods as SHG or Pockels effect, where explicit knowledge of the hyperpolarizability of the chromophore within the matrix as well as of the local field correction factors is necessary to calculate absolute values of the polar order parameters, these properties are not relevant using measurements of the linear and the quadratic Stark effect.

The Stark effect is the the shift of the wavenumber $\tilde{\nu}$ of the optical absorption band of a chromophore with fixed orientation in a polymeric matrix in an electric field E by

$$\frac{h}{c}\Delta\tilde{\nu} = -\Delta\bar{\mu}\ \bar{E} -\tfrac{1}{2}\left(\Delta\bar{\alpha}\ \bar{E}\right)\bar{E} \tag{1}$$

where $\Delta\bar{\mu} = \bar{\mu}_e - \bar{\mu}_g$, $\Delta\bar{\alpha} = \bar{\alpha}_e - \bar{\alpha}_g$, $\bar{\mu}_g$, $\bar{\mu}_e$ are dipole moments and $\bar{\alpha}_g$, $\bar{\alpha}_e$ polarizabilities in the ground and excited state, respectively. In experiments however, it's easier to measure the change of the absorbance ΔA of a sample at fixed wavelengths instead of $\Delta\tilde{\nu}$. After description of ΔA as a Taylor series of the curve $(A/\tilde{\nu})$ and averaging over all molecular orientations present in the sample, one gets for the field induced change in absorption of typical rod like NLO molecules like stilbene or azobenzene chromophores, where $\Delta\bar{\mu}$ as well as the transition dipole moment $\bar{\mu}_{ge}$ can be considered as collinear to the molecular long axis, (the electric field is parallel to the direction of the light propagation, the anisotropy of $\Delta\bar{\alpha}$ is neglected) [6-8]

$$\langle\Delta A\rangle = \frac{3}{2}\frac{\Delta\mu E}{hc}\tilde{\nu}\frac{\partial(A/\tilde{\nu})}{\partial\tilde{\nu}}\langle\cos\theta\sin^2\theta\rangle +$$
$$\frac{1}{2}E^2\left[\frac{\Delta\alpha}{hc}\tilde{\nu}\frac{\partial(A/\tilde{\nu})}{\partial\tilde{\nu}}+\frac{3}{2}\left(\frac{\Delta\mu}{hc}\right)^2\tilde{\nu}\frac{\partial^2(A/\tilde{\nu})}{\partial\tilde{\nu}^2}\langle\cos^2\theta\sin^2\theta\rangle\right]. \tag{2}$$

The linear effect (first term in (2)) will only occur in polar samples and is sensitive to the order parameter $<\cos\theta\sin^2\theta>$, whereas the quadratic effect (second term in (2)) will also be observed in unpolar media.

The modulation technique used (i. e. $E = E\sin\omega t$) allows for the measurement of ΔA by lock-in technique. Since the response to E^2 occurs at DC and 2ω only, it is possible to distinguish between the linear and the quadratic effect measuring ΔA at the ω or 2ω, respectively. Considering effective values for ΔA and E, the quadratic-in-field absorption change of an isotropic sample (here $<\cos^2\theta\sin^2\theta> = 2/15$) is given by

$$\Delta A_{qu}^{eff}(2\omega) = \frac{1}{\sqrt{2}}E_{eff,loc}^2\left[\frac{\Delta\alpha}{2hc}\tilde{\nu}\frac{\partial(A/\tilde{\nu})}{\partial\tilde{\nu}}+\frac{(\Delta\mu)^2}{10h^2c^2}\tilde{\nu}\frac{\partial^2(A/\tilde{\nu})}{\partial\tilde{\nu}^2}\right] \tag{3}$$

Thus the quadratic effect of an unpoled sample allows for the measurement of $\Delta\mu$, which may be used to calculate the order parameter $<\cos\theta\sin^2\theta>$ from measurements of the linear effect:

$$\Delta A_{lin} = \frac{3}{2}\frac{\Delta\mu E_{eff}^{loc}}{hc}\tilde{\nu}\frac{\partial(A/\tilde{\nu})}{\partial\tilde{\nu}}\langle\cos\theta\sin^2\theta\rangle \tag{4}$$

In the case of limited poling field strength, the approximation $<\cos\theta\sin^2\theta> \approx \frac{2}{5}<\cos\theta>$ is valid. If the same modulation frequency is applied, identical correction factors have to be used for both linear and quadratic effect to calculate the local field E_{eff}^{loc} from the external field E_{eff}. Thus, the the value $<\cos\theta\sin\theta>$ obtained is *independent* of the model used for the local field correction.

Experimental

Thin films (typically 2 μm) of polymeric guest/host systems with the azo dye DMANA, the stilbene dye DEANS and the biphenyl dye DMANB (figure 1) in polycarbonate bisphenol-A with a concentration of about 2 % per weight were prepared on ITO coated glass substrates using spin coating from a solution in cylopentanone. After heating of the films under vacuum to remove solvent, semi-transparent gold electrodes were sputtered onto the film surface. For photoassisted poling the films were illuminated by visible light from a 250 W halogene lamp filtered with infrared filters (5 cm water, Schott KG 4) and a color glass filter to the absorption band of the chromophore. Absorption spectra in the visible range were measured with a Cary 17 spectrometer. Stark spectra were taken using a home build spectrometer with a photomultiplier as detector. Electric field with a frequency of 333 Hz was applied to the samples and the AC component $\Delta I(\lambda,E)$ of the optical transmission was detected with a lock-in amplifier. Equations (3,4) were fitted to the spectra $\Delta A(\lambda,E)$ to evaluate $\Delta\alpha$, $\Delta\mu$ and subsequently $<\cos\theta>$.

Results and Discussion

Poling time dependence of induced polar order: To be sure to reach equlilibrium poling conditions we measured the linear Stark effect after poling of the film, varying the polin duration and switching off poling voltage and light at the same time. We found no significant difference in the order parameter after 30 up to 120 min poling. Thus 30 min poling time is sufficient to reach equilibrium. The behavior was similar for all investigated dyes.

A difference in the behaviour is observable, if the poling voltage is applied longer than the light exposure: The polar order parameter of the azo dye containing film is increased about 4 times in experiments where the poling field is applied 15 min longer than illumination compared to experiments where poling voltage and light are switched off simultaneously. This enhancement is more than described in experiments on an azo side-chain polymer [2] but in accordance to theoretical considerations [4], where the poling is attributed to the cis isomer with a certain orientational memory after the thermal relaxation to the trans isomer. As described earlier [3] and established experimentally by absorption spectroscopy the thermal relaxation cis⇒ trans is finished after several minutes.

Intensity dependence of polar order: The polar order parameter of azo and stilbene containing films was measured after photoassisted poling (30 min illumination, 30+15 min application of poling field) with different intensities of light. The result for DMNA is shown in figure 2. According to [4] the polar order parameter should be proportional to the number density of the cis isomer during illumination, which is governed by the thermal relaxation time τ_{th} and the mean temporal difference τ_p between two trans⇒cis transitions, the latter is inverse proportional to the light intensity. Indeed a fit to the equation $<\cos\theta>=<\cos\theta>_\infty/(1+\tau_p/\tau_{th})$ following from this model (and shown as straight line in figure 2) gives a value $\tau_{th} = 4$ s in agreement with literature [3] (τ_p was calculated from the light intensity and the absorbance of the film). Surprisingly, because the model mentioned above cannot be applied to this systems, we found a similar behaviour in the lower intensity range for the films containing stilbene dyes. Measurements in the higher intensity range are in progress.

Comparison of order parameters obtained from different dyes: The photoassisted poling of stilbene and biphenyl dye containing films cannot be explained by a trans⇔cis isomerization cycle, since stilbene shows no thermal relaxation cis⇒trans and for biphenyl no isomerization is possible at all. Thus heating of the polymer film must be considered: Measurements and theoretical estimations have shown that the film temperature is raised by about 2 K during illumination with 200 mW/cm^2. It's evident from measurements of $<\cos\theta>$ as function of poling temperature (cf. figure 3) that this temperature difference is not sufficient to explain the induced polar order during photoassisted poling. Thus we believe that a local heating of a molecule and its vicinity enhances the rotational mobility of the molecule and allows for a more pronounced polar orientation of the dipoles than without illumination. Table 1 shows a comparison of order parameters normalized to the values anticipated from a Boltzmann distribution of dipoles (in a free gas model) in the poling field measured at different systems. For stilbene and azo dyes we find identical behaviour, thus photoisomerization of stilbene doesn't influence the poling. In a poling procedure where light and poling field are switched off simultaneously DEANS and DANB reach almost half of the polar order of the azo dye DMANA. Thus one can conclude that even for azo dyes local heating must be considered in a theoretical description of the process.

Very efficient photoassisted poling, comparable to the efficiency of thermal poling close to the glass transition, is only possible with the azo dye. Here a poling procedure where the field application exceeds light exposure for several minutes until the thermal relaxation cis⇒trans is finished must be used.

Acknowledgment

References

[1]   Z. Sekkat and M. Dumont, *Appl. Phys. B*, **54**, 486 (1992).

[2]   Z. Sekkat and M. Dumont, *Synthetic Metals*, **54**, 373 (1992).

[3]   R. Loucif-Saïbi, K. Nakatani, J. A. Delaire, M. Dumont, and Z. Sekkat, *Chem. Mater.*, **5**, 229 (1993).

[4] Z. Sekkat and W. Knoll, *J. Opt. Soc. Am. B* (in press).

[5] L. M. Blinov, M. I. Barnik, T. Weyrauch, S. P. Palto, A. A. Tevosov, and W. Haase, *Chem. Phys. Lett.*, **231**, 246 - 252 (1994).

[6] M. I. Barnik, L. M. Blinov, W. Haase, S. P. Palto, A. A. Tevosov, and T. Weyrauch, in *Nonlinear Optical Polymers: From Molecules to $\chi^{(2)}$ Applications*, ACS Symposium Series, Eds. G. A. Lindsay and K. D. Singer, in press.

[7] M. I. Barnik, L. M. Blinov, S. P. Palto, A. A. Tevosov, and T. Weyrauch, *Mol. Mat.*, **3**, 319 (1994).

[8] W. Liptay, in *"Modern Quantum Chemistry"*, ed. O. Sinanoglu, v.3, Academic Press, NY, 1965, p. 45.

DMANA   DEANS   DMANB
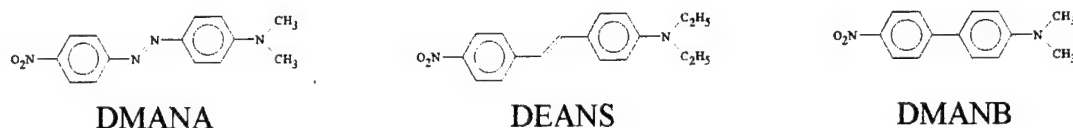
Figure 1: Structure of the investigated dye molecules
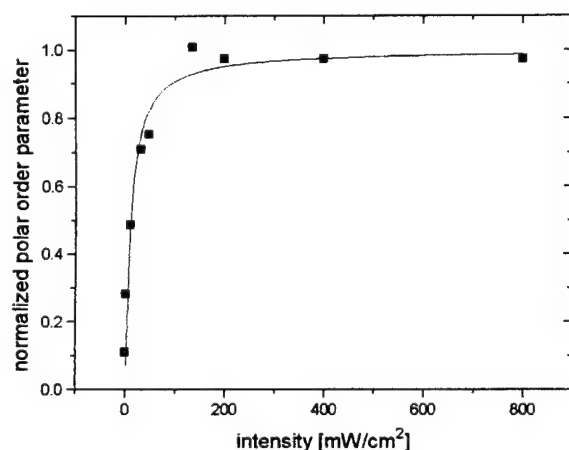

Figure 2: Dependence of the polar order parameter <cosθ> as function of light intensity during photoassisted poling at room temperature (30 min illumination, 30+15 min application of poling field)
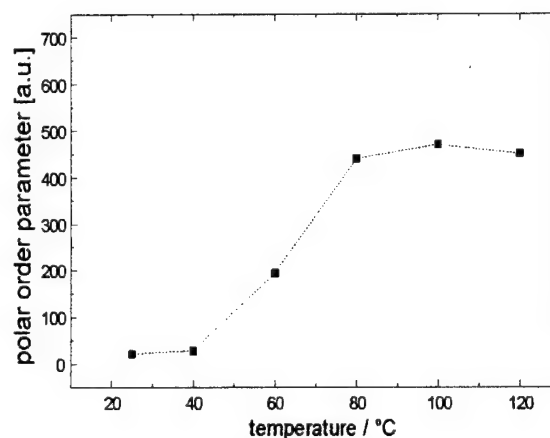
Figure 3: Dependence of the polar order parameter <cosθ> as function of poling temperature in a poling procedure without illumination

Poling procedure	DMANA	DEANS	DMANB
30 min, 200mW/cm² field and light switched off simultaneously	6 %	2,4 %	2,5 %
30 min illumination, 200mW/cm², 30+15 min field application	26 %	4 %	-

Table 1: Polar order parameters <cosθ> normalized to the value <cosθ>=$\mu E/5kT$ anticipated from Boltzmann distribution of dipoles μ in the poling field E.

Coherent Detection of Freely Propagating Terahertz Radiation by Electro-optic Sampling in a Poled Polymer

Ajay Nahata[a], Tony F. Heinz[a], David H. Auston[a,c], and Chengjiu Wu[b]

(a) Department of Electrical Engineering, Columbia University, New York, NY 10027

(b) AlliedSignal Inc., Research and Technology, P.O. Box 1021, Morristown, NJ 07960

(c) Current Address: Office of the Provost, Rice University, Houston, TX 77005

Electronic Mail: an23@columbia.edu ; Tel.: (212) 854-3137; Fax: (212) 854-1909

Abstract.

We report the first demonstration of an electro-optic sampling technique that allows for the coherent detection of freely propagating terahertz radiation.

Coherent Detection of Freely Propagating Terahertz Radiation by Electro-optic Sampling in a Poled Polymer

Ajay Nahata[a], Tony F. Heinz[a], David H. Auston[a,c], and Chengjiu Wu[b]

(a) Department of Electrical Engineering, Columbia University, New York, NY 10027

(b) AlliedSignal Inc., Research and Technology, P.O. Box 1021, Morristown, NJ 07960

(c) Current Address: Office of the Provost, Rice University, Houston, TX 77005

Electronic Mail: an23@columbia.edu ; Tel.: (212) 854-3137; Fax: (212) 854-1909

The use of ultrafast laser sources to generate and detect freely propagating pulses of coherent far-infrared radiation (FIR) has stimulated significant interest in recent years. Terahertz (THz) bandwidth pulses are typically generated by exciting radiative current transients in photoconductive media [1,2] or producing a nonlinear polarization via difference frequency mixing in nonlinear optical media [3]. To date, the only broadly applicable technique to coherently detect this radiation requires the use of synchronously gated photoconducting dipole detectors [1,2]. While these detectors exhibit excellent sensitivity, there is a strong speed versus sensitivity trade-off which is determined by the photoconductive response and antenna dimensions [4].

Electro-optic sampling [5] has been used extensively to study ultrafast electrical pulses. A significant advantage of this technique is the potential of increasing the detection bandwidth to that of the optical probe bandwidth. This is especially true with the use of poled polymers, where the material response time is negligible [6]. However, this technique has been primarily limited to transmission line and circuit characterization.

In this submission, we describe the first demonstration, to the best of our knowledge, of an electro-optic sampling technique that allows for the coherent detection of freely propagating sub-millimeter wave radiation. In our setup, the emitter and detector are physically separated by a large distance. The electro-optic sampling is performed in a poled polymer, which we designate MA9:MMA. The chemical structure and linear and nonlinear optical properties are described elsewhere [7]. In these preliminary results, we show that the poling electrodes diffract the incident electric field. We discuss the effect on the temporal waveform and ways to eliminate the effect.

We fabricated the electro-optic sampling element (EOSE) on an R-plane sapphire substrate. A high reflectivity dielectric coating centered at 800 nm was first evaporated onto one side of the substrate. Two coplanar 5 mm x 5 mm aluminum pads separated by 50 μm, used for poling, were then photolithographically defined onto the coating. A 10 μm thick film of the copolymer was then cast from solution, baked at 130° C for 3 hours, and poled with a 1.0 MV/cm field. A silicon lens [4] was attached to the sapphire substrate to focus the THz radiation into the electrode gap.

The experimental setup for generating and detecting THz radiation is shown in Figure 1. A mode-locked Ti:sapphire laser operating at 800 nm was used to generate and detect the transient sub-millimeter wave pulses. A 400 mW pump was chopped at 95 kHz

and used to drive a large aperture photoconducting antenna. This antenna was biased so that the resulting THz radiation was polarized parallel to the c-axis of the poled polymer. A pair of off-axis paraboloidal mirrors were used to collimate and focus the THz radiation into the EOSE.. The total separation between the emitter and detector was 60 cm. The detection system employed a crossed polarizer arrangement with differential detection [5].
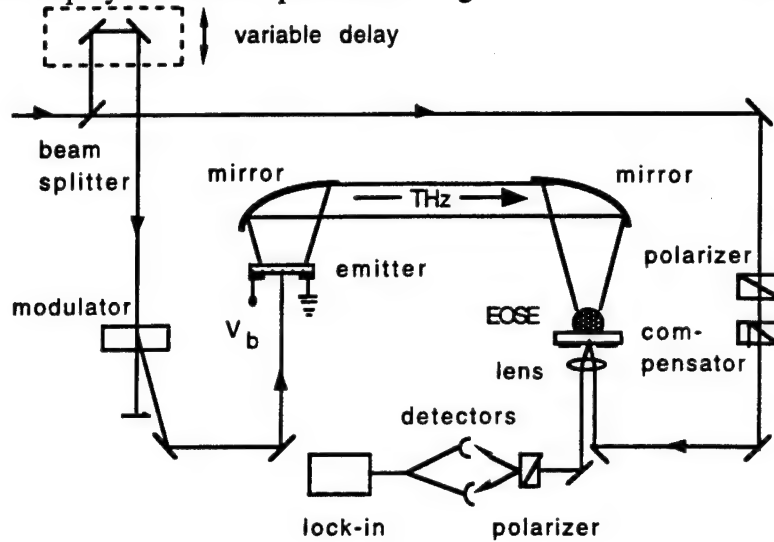

Figure 1

In the small angle approximation, the double pass phase retardation can be related to the electro-optic coefficient r_{33} by $\Delta\Gamma \approx 4\pi\ell n^3 r_{33}E/3\lambda$, where $n_o \approx n_e = n = 1.65$, n_o and n_e are the ordinary and extraordinary refractive indexes, respectively, ℓ is the polymer thickness, λ is the wavelength of the optical probe, and E is the applied field. Since the poling field is relatively low, we also assume $r_{33} \approx 3r_{13}$. The observed low frequency (95 kHz) electro-optic coefficient r_{33} was determined to be 11 pm/V corresponding to a value of E_π, the field needed to cause a π phase retardation, of 12 MV/cm. For square wave amplitude modulation of the electric field, the rms signal current from the receiver at the chopping frequency is $i_{sig} = 2\sqrt{2}I_oE(t)/E_\pi$, where I_o is the quiescent current from each detector and E(t) is the electric field. The total shot noise of the photodiode quiescent current is $i_{SN} = \sqrt{4qI_oB}$, where q is the electron charge and B is the detection bandwidth. In the shot noise limit, the minimum detectable field occurs when $i_{sig}=i_{SN}$, so that $E_{min} = E_\pi\sqrt{q/2I_o}$ (V/cm)/$\sqrt{Hz}$. Thus, for a quiescent current of 1 mA and 1 Hz bandwidth, the minimum detectable field is 107 (mV/cm)/$\sqrt{Hz}$.

The temporal response of the system with an antenna bias of 300 V is shown in figure 2. We calibrated the THz response of the EOSE by applying a bias across the 50 μm electrode gap. Such a calibration requires that we neglect the difference in field distributions between the diffracted THz field and the fringing applied voltage. We also neglect the dispersion of the electro-optic coefficients. The peak detected field was found to be ~18 V/cm with a noise floor of 2.9 (V/cm) /$\sqrt{Hz}$.
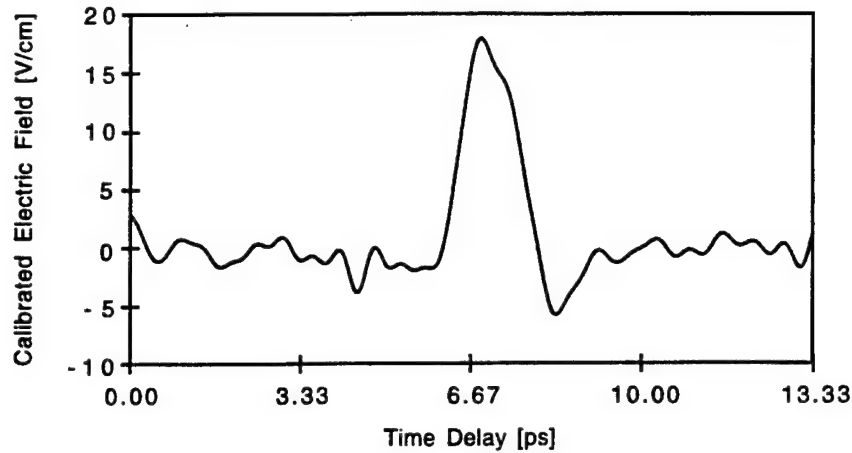
Figure 2

In the far field, the radiated electric field is expected to have a bipolar shape, such that total time integral is zero [2]. The observed shape of the detected waveform in Figure 2, however, is unipolar. This effect is caused by diffraction of the incident THz field induced by the metal electrodes in the EOSE. The diffracted field may be modeled by classical electromagnetic diffraction through a 2-dimensional conducting screen with a narrow slit [8]. To first order, the diffracted field (and corresponding electrode voltage) is proportional to the time integral ($\omega^{-1}E(\omega)$) of the incident field. Thus, an approximate expression for the voltage across the slit can be written as [1]

$$v_s(t) = \frac{1}{Z_o C_s} \int_{-\infty}^{t} dt' E_i(t')$$ (1)

where Z_o is the characteristic impedance of the medium and C_s, which has a weak frequency dependence, is the static capacitance of the electrode structure per unit length.

We demonstrate the integrating nature of the EOSE by using a 100 µm Hertzian dipole detector that has been shown to preserve the bipolar nature of the incident field [4]. Figure 3 shows the detected waveform with the dipole detector substituted for the EOSE with all other experimental parameters unchanged. As expected, this waveform is bipolar. The time integral of this signal is shown in Figure 4. While the waveform shapes of Figure 2 and 4 are very similar, the FWHM time of the former signal is smaller. This is due to the fact that the overall FWHM detection response time τ_s of the EOSE is < 200 fs, which is smaller than that of our dipole detector.

It should be possible to modify the sampling element so that the incident field is not integrated. This can be accomplished by removing the electrodes after poling or by using an appropriate organic single crystal. Further reduction of the minimum detectable field should be possible by performing the experiment in a transmission geometry. Here, the THz field would again be normally incident on the EOSE. The probe beam, however, would be incident at the phase velocity matching angle. This angle is relatively small in polymers due to the low refractive index dispersion [9]. The probe beam, therefore,

copropagates with the THz beam allowing for longer interaction lengths. These ideas are currently being investigated.
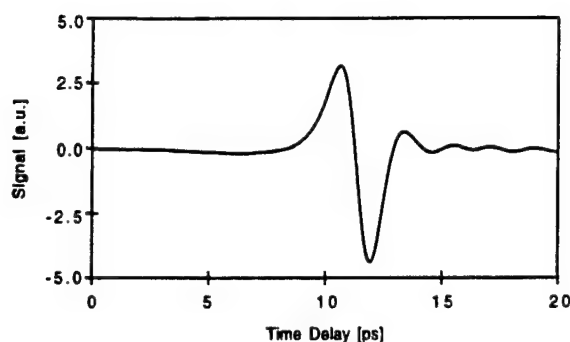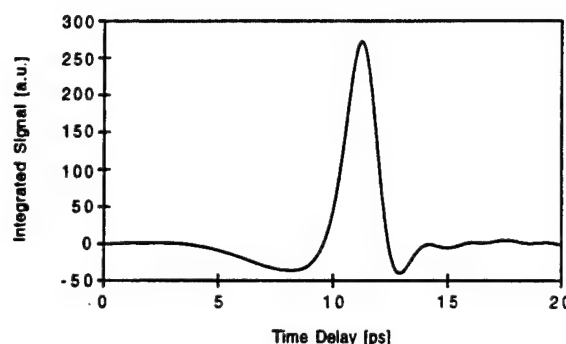

Figure 3

Figure 4

In conclusion, we have demonstrated an electro-optic sampling technique that allows for the coherent detection of freely propagating THz radiation. This geometry is amenable to applications such as THz time-domain spectroscopy. With appropriate changes in the sampling element and sampling geometry and by using polymers with an electro-optic coefficient r_{33} on the order of 60 pm/V [10], it should be possible to significantly increase the detection sensitivity and maintain extremely low response times.

This research was supported by the Air Force Office of Scientific Research under grant F49620-92-J-0036.

References:

[1] D.H. Auston, K.P. Cheung, and P.R. Smith, Appl. Phys. Lett. **45**, 284 (1984).

[2] P.R. Smith, D.H. Auston, and M.C. Nuss, IEEE J. Quant. Electron. **24**, 255 (1988).

[3] B.B. Hu, X.-C. Zhang, D.H. Auston, and P.R. Smith, Appl. Phys. Lett. **56**, 506 (1990).

[4] D. Grischkowsky, in *Frontiers in Nonlinear Optics*, edited by H. Walther, N. Koroteev, and M.O. Scully (Institute of Physics Publishing, Philadelphia, 1992) and references therein.

[5] J.A. Valdmanis, G.A. Mourou, and C.W. Gabel, Appl. Phys. Lett. **41**, 211 (1982).

[6] P.M. Ferm, C.W. Knapp, C. Wu, J.T. Yardley, B.B. Hu, X.-C. Zhang, and D.H. Auston, Appl. Phys. Lett. **59**, 2651 (1991).

[7] C. Wu, K. Beeson, P. Ferm, C. Knapp, M. McFarland, A. Nahata, J. Shan, and J.T. Yardley, Mat. Res. Soc. Symp. Proc. **328**, 477 (1994).

[8] C.J. Bouwkamp, Rep. Progr. Phys. **17**, 35 (1954).

[9] A. Nahata, D.H. Auston, C. Wu, and J.T. Yardley, Appl. Phys. Lett., in press.

[10] Y.M. Cai and A. K-Y. Jen, Appl. Phys. Lett. **67**, 299 (1995).

Real and imaginary components of the third-order nonlinearity of polyaniline dodecylbenzenesulfonic salt

M. Samoc, A. Samoc, B. Luther-Davies, J. Swiatkiewicz[*] , C. Q. Jin and J. W. White

Laser Physics Centre, Research School of Physical Sciences and Engineering, and Research School of Chemistry,
The Australian National University, Canberra, ACT 0200, Australia

Abstract

The third-order optical nonlinearity of a salt of polyaniline has been measured at 527 nm, 800 nm and 1054 nm: the dominant nonlinear response being absorption bleaching giving high negative values of the imaginary part of n_2.

Real and imaginary components of the third-order nonlinearity of polyaniline dodecylbenzenesulfonic salt

M. Samoc, A. Samoc, B. Luther-Davies, J. Swiatkiewicz*) , C. Q. Jin and J. W. White

Laser Physics Centre, Research School of Physical Sciences and Engineering, and Research

School of Chemistry,

The Australian National University, Canberra, ACT 0200, Australia

There have been several reports of the third-order nonlinear optical properties of polyaniline (PANI) with most experiments carried out using the base form of the material [1-6]. Recently, Petrov *et al* [7] published results for a composite film containing the salt form of polyaniline for which both the real (refractive) and imaginary (absorption bleaching) parts of the nonlinearity were evaluated from Z-scan measurements at 532 nm using Q-switched trains containing several 70 ps duration pulses. They concluded that the nonlinear optical properties of polyaniline and specifically the ratio of n_2/α, n_2 being the nonlinear refractive index and α being the linear absorption coefficient, were attractive for applications in all-optical switching.

We report measurements of the nonlinearity of a particular form of PANI - the salt of polyaniline with dodecylbenzenesulfonic acid (DBSA). The absorption spectrum of DBSA-PANI has its main peak close to 800 nm (Figure 1) and is similar to that of the form of PANI investigated in [7]. The DBSA counterion was used to improve the solubility of PANI and its miscibility with host polymer materials [8]. Measurements of the nonlinear optical properties in solution used N-methylpyrrolidone (NMP) as the solvent. Films of a composite of PANI with polymethylmethacrylate (PMMA) were also used for some measurements.

The nonlinear optical measurements were performed at 527, 800 and 1054 nm. A Coherent MIRA Ti:sapphire oscillator and a regenerative amplifier running at 30Hz was used to generate 100fs duration pulses containing up to 1mJ of energy at 800nm. A Coherent Antares Nd:YLF laser and regenerative amplifier running at 1-20Hz was used to generate single pulses at 1054nm or 527nm (with a KDP frequency doubler) at durations between 7 and 35ps. Degenerate four wave mixing, time resolved pump-probe measurements, and the Z-scan technique were used to obtain data on the optical nonlinearity.
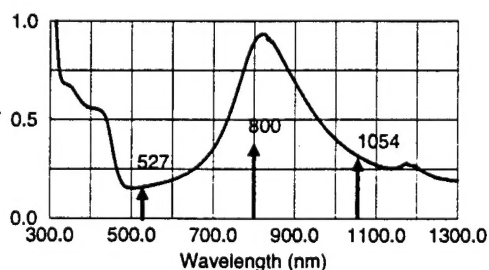

Figure 1: Optical density of ≈0.37% solution of PANI-DBSA in N-methylpyrrolidone measured in a 1mm glass cell. The arrows indicate wavelengths used for the nonlinear optical measurements.

Figure 2 shows a time-resolved degenerate four-wave mixing signal obtained at 800 nm

for a free standing film of PMMA/PANI composite. Similar to the results obtained at 620 nm reported in [3], there is an instantaneous component of the nonlinear response accompanied by a slow component appearing as a relatively well pronounced tail in the DFWM signal with a decay time of $\approx$5ps. The effective nonlinearity $|n_2|$ was calculated from the DFWM signals from the PANI composites against a fused silica reference. For samples containing a few percent of PANI $|n_2|$ lay in the range 10^{-14}–10^{-13} c m^2/W. Since samples of different concentrations were studied, a more relevant parameter is the ratio $|n_2|/\alpha$. which should be concentration independent. For the PMMA/PANI films this ratio was typically 10^{-16} cm^3/W, however, a relatively large scatter of the results was observed (by as much as an order of magnitude) due largely to the large corrections that must be applied to the data to account for the linear absorption in the films. (The effect of the bleaching described below was not taken into account in making these corrections.)
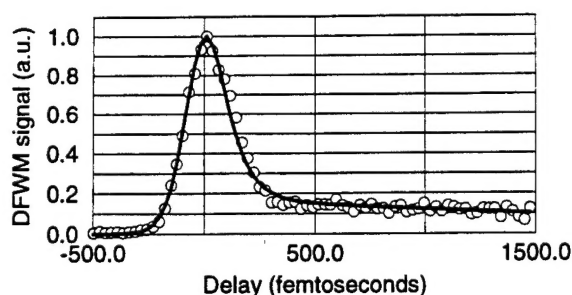

Figure 2: A degenerate four-wave mixing scan for a free-standing film of PMMA doped with PANI(circles) at 800 nm and a theoretical fit (full line) . The laser intensity was 30GW/cm^2.

To evaluate the role of absorption bleaching we performed time-resolved pump-probe measurements at 800 nm (Figure 3). The bleaching response also contains two components: an instantaneous change attributable to the optical Stark effect (ie. modification of the absorption coefficient by the laser field) and a slowly decaying component possibly due to a presence of a relatively long lived excitation. From these results we determined the nonlinear absorption coefficient β (defined by $\alpha=\alpha_0+\beta I$) to be $\beta\approx- 4\times10^{-10}$ cm/W (for the 2% doped films).
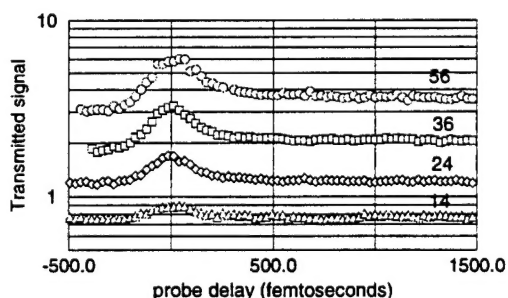

Figure 3: Induced transmission in a sample of PMMA/PANI (about 2 %) at a few pump intensities given in the picture (in GW/cm^2, the probe intensity was a constant fraction ~ 25% of the pump intensity.)

Because of the relatively large scatter of values determined from DFWM it was not practical to compare the magnitudes of the real and imaginary components of the nonlinearity by combining the DFWM data with the bleaching data. Instead, we resorted to Z-scan measurements. Using the formalism presented in [9] we fitted the experimental Z-scan

profiles to obtain information on the real and imaginary parts of the nonlinearity. Figure 4 shows Z-scan data obtained at 800 nm for a set of NMP solutions with different concentrations of DBSA-PANI.
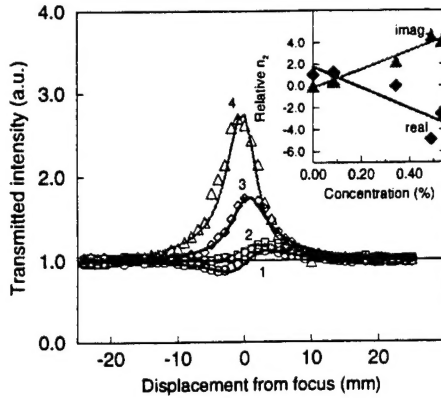

Figure 4 : Closed-aperture Z-scan measurements performed using 100 fs pulses at 800 nm on a series of PANI-DBSA solutions in N-methylpyrrolidone. The insert shows concentration dependencies of the real and imaginary part of the nonlinearity of the solution relative to the nonlinearity of the pure solvent. 1- pure solvent, 2- 0.086%, 3- 0.34% 4- 0.53% of PANI-DBSA in NMP.

It is apparent that at higher concentrations of the solute the Z scans become dominated by the bleaching effect. At the same time, however, the real part of the nonlinearity of the solution changes from positive for low PANI concentration to negative at high PANI concentration. This means that the real part of n_2 for PANI is negative. The same sign for the refractive nonlinearity was also obtained from Z-scan measurements at 1054 nm. However at 527 nm the refractive nonlinearity was found to be positive.

Table 1 summarises the data for the three wavelengths. All values have been calculated assuming that the nonlinear refractive index n_2 of the solvent N-methylpyrrolidone was 1.5×10^{-15} cm^2/W at all wavelengths, which is the average from our various measurements of this parameter using Z-scans or DFWM referenced against fused silica. Note the values have been extrapolated to 100% PANI from our values for low concentration solutions. The values of $|Re(n_2)/\alpha|$ were calculated from these data thereby taking the absorption of the different PANI solutions into account.

The ratio n_2/α can be related to the merit factor W used to compare the properties of nonlinear media in which the nonlinear phase change is limited by single-photon absorption [10]. W is defined as $\Delta n_{max}/\alpha\lambda$ where Δn_{max} is the maximum obtainable refractive index change and λ is the wavelength. Operation of a nonlinear directional coupler requires W>2. Since $\Delta n_{max} = n_2 I_{sat}$ where I_{sat} is the light intensity at which the refractive index change saturates, one can present W as $n_2 I_{sat}/(\alpha\lambda)$. For comparison with data presented by Stegeman in [10] we assumed $I_{sat} = 1$ GW/cm^2. For 800 nm this results in W=0.007: a very poor performance indicator. We conclude, in contrast to Petrov *et al* [7], that PANI is not a promising material for use in all-optical switching.

Some of the discrepancy between our results and those in [7] could be due to differences in the chemical character of the materials. Nevertheless, measurements we have made on other forms of PANI did not give values significantly different than those reported here. More important in explaining the discrepancy is likely to be our use of single, high contrast pulses

and weak focussing into the samples in comparison with the pulse trains and tight focussing used in [7]. Our measurements are less susceptible to errors due to thermal nonlinearities; the creation of long lived excited states (which can contribute accumulative effects when probed by a pulse train); and permanent bleaching. Confusing contributions from several of these sources were in fact observed during, and eliminated from, our measurements.

Table 1: Real and imaginary parts of the third-order nonlinearity of PANI-DBSA in N-methylpyrrolidone solutions obtained from Z-scan measurements. The data is extrapolated to 100% PANI from data obtained from low concentration solutions.

Wavelength (nm)	$Re(n_2)$ (cm^2/W)	$Im(n_2)$ (cm^2/W)	β (cm/W)	$|Re(n_2)/\alpha|$ (cm^3/W)
527	5.9×10^{-13}	-2.9×10^{-13}	-6.8×10^{-8}	4.3×10^{-16}
800	-1.4×10^{-12}	-1.3×10^{-12}	-2.1×10^{-7}	2.5×10^{-16}
1054	-1.7×10^{-12}	-3.5×10^{-13}	-4.2×10^{-8}	7.4×10^{-16}

REFERENCES

1. C. Halvorson, Y. Cao, D. Moses and A.J. Heeger, Synth. Met. **57**, 3941 (1993)

2. J.A. Osaheni, S.A. Jenekhe, H. Vanherzeele, J.S. Meth, Y.Sun and A.G. MacDiarmid, J.Phys.Chem.**96**, 2830 (1992)

3. W.C. Chen, S.A. Jenekhe, J.S. Meth and H. Vanherzeele, J.Polym.Sci. Part B, Polym.Phys. **32**, 195 (1994)

4. K.S. Wong, S.G. Han and Z.V. Vardeny, J. Appl.Phys. **70**, 1896 (1991)

5. K.S. Wong, S.G. Han and Z.V. Vardeny, Synth.Metals, **41-43**, 3209 (1991)

6. K.S. Wong and Z.V. Vardeny, Synth.Met. **49**, 13 (1992)

7. D.V. Petrov, A.S.L. Gomes, C.B. de Araujo, J.M. de Souza, W.M. de Azevedo, J.V. de Melo and F.B. Diniz, Optics Lett. **20**, 554 (1995).

8. Y. Cao, P. Smith and A.J. Heeger, Synth. Metals, **55**, 3514 (1993)

9. M. Sheikh-bahae, A.A. Said, T. Wei, D.J. Hagan and E.W. van Stryland, IEEE Journ. Quantum Electr., **26**, 760 (1990)

10. G.I. Stegeman in: Contemporary Nonlinear Optics, Academic Press 1992, p.22-23

*) on leave from Photonics Research Laboratory, State University of New York at Buffalo, NY